Journal of Molecular Modeling (2023) 29:163
https://doi.org/10.1007/s00894-023-05561-0

ORIGINAL PAPER

Insight into the addition reactions of stannylenoid H_2SnLiF with ethylene

Shuo Wu[1] · Bingfei Yan[1] · Shaoli Liu[1] · Wenzuo Li[1]

Received: 3 February 2023 / Accepted: 16 April 2023 / Published online: 28 April 2023

Abstract

Context Tetrylenoids, R_2EXM (E = Si, Ge, and Sn; X = electronegative group; M = alkali metal), have electrophilic and nucleophilic properties just like carbenoid. As the products of carbenoid compounds with olefins, the cyclopropane fraction has been found to be biologically active in many natural and artificial compounds. Can carbenoid analogues of stannylenoid facilitate similar cyclopropanation reactions?

Methods Addition reaction of the stannylenoid compound H_2SnLiF with ethylene was investigated using density function theory (DFT) at the M062X/def2-TZVP level. The single-point energy calculations were performed on the basis of QCISD/def2-TZVP level.

Results Two possible pathways were found for the addition reaction of H_2SnLiF (R1) with ethylene (R2). The most favorable path is the two successive reactions of H_2SnLiF and ethylene through the ternary ring product c-$H_2Sn(CH_2)_2$ (P1) and then the formation of the five-membered ring product (P2). Solvation-related studies have shown that addition reactions are more likely to occur in the presence of THF solvents. This work provides theoretical support for the reactions of stannylenoid with olefins.

Keywords H_2SnLiF · Ethylene · Addition reaction · DFT

Introduction

Tetrylenoids, R_2EXM (E = Si, Ge and Sn; X = electronegative group; M = alkali metal), are heavier homologues of carbenoid compounds [1, 2], which have electrophilic and nucleophilic properties just like carbenoid. Silylenoids and germylenoids have been successfully synthesized and isolated over decades of exploration, and their structures and reaction properties have been well investigated experimentally and theoretically [3–26].

Stannylenoid is a class of tetrylenoids with the structural general formula R1R2SnXM, which is an active intermediate. Scientists have also reported on their structure and synthesis. Grugel [27] team was the first to predict the existence of stannylenoid compounds in the reaction of aldehyde with some stannylene precursors. Then, Arif et al. [28] and Ochiai et al. [29] successfully isolated the stannylenoid compounds and observed their structures by X-ray diffraction. Yan et al. [30] used the corresponding stannylenes to react with cesium fluoride to synthesize stable stannylenoid for the first time. Then Gross et al. [31] found that free stannylene can be obtained through stannylenoid. Subsequently, some experiments also confirmed this conclusion [32, 33].

Zhao et al. [34] reported the reaction of dipotassium-tetrasilyl-1,4-dioxide with anhydrous $SnCl_2$ to form a five-membered cyclic potassium chlorostannate, which was converted to chlorinated stannylenoid by a cation exchange reaction. Then, Yan et al. [35] reported a variety of reactions of fluorinated stannylenoid with acetylene and showed unique reactivity to acetylene with alkynyl hydrogen and acetylene with trimethylsilyl group. Recently, Zhao et al. [36] reported a new stannylenoid which was obtained by the reaction of lithium aryl(silyl)amide with an equivalent amount of $SnCl_2$ in THF, and studied its reactivity.

✉ Shaoli Liu
liushaoli6984@sina.com

✉ Wenzuo Li
liwenzuo2004@126.com

[1] The Laboratory of Theoretical and Computational Chemistry, School of Chemistry and Chemical Engineering, Yantai University, Yantai 264005, People's Republic of China

The addition reactions of carbenoid compounds with olefins have been extensively studied [1, 37–41], and the cyclopropane fraction of their products has been found to be biologically active in many natural and artificial compounds. Can carbenoid analogues of stannylenoid facilitate similar cyclopropanation reactions? This is a noteworthy topic not only for experimental researchers but also for theoretical ones. Therefore, this work will explore the reaction of stannylenoid with olefins using the simplest stannylenoid, H_2SnLiF, to react with ethylene and clarify the reaction mechanism. The results of this work would provide a theoretical basis for the subsequent generation of tin-containing compounds.

Theoretical methods

Geometries of the stationary points on the potential energy surface were first optimized using the DFT [42, 43] M062X method and the def2-TZVP basis set, and then harmonic vibrational frequencies were calculated at the same level for characterizing the minimum or first-order saddle point of the optimized geometry. To improve the treatment of electronic correlations, the single-point energies of all stationary points were calculated at the def2-TZVP level of theory using the QCISD [44] method. Unless otherwise stated, the relative energies given in this paper are those calculated at the QCISD/def2-TZVP//M062X/def2-TZVP levels, including the (scale-free) correction for the zero-point vibrational energy measured at the M062X/def2-TZVP level. The mechanism of the addition reaction was verified by intrinsic reaction coordinate (IRC) analysis of the possible transition states (TS) to demonstrate that each TS correctly connects the corresponding precursor complex (Q) to the product (P). To account for solvent effects, the geometry and energy of the stationary point in the addition reaction was calculated using the SMD model [45], and the tetrahydrofuran (THF) solvent was chosen (dielectric constant $\varepsilon = 7.4$). We used Multiwfn and VMD software to draw frontier molecular orbitals [46, 47]. All calculations were performed using the Gaussian 09 [48] series of programs.

Table 1 The relative energies (kJ/mol) of each stable configuration of H_2SnLiF in vacuum and THF are calculated at the QCISD/def2-TZVP//M062X/def2-TZVP level

	Vacuum	THF
P-complex	0.00	0.00
Three-membered ring	36.34	4.19
"Classical" tetrahedral	112.28	54.64

Results and discussions

Structure of H_2SnLiF

First, we calculated all the stable structures of H_2SnLiF on the basis of M062X/def2-TZVP. The results indicated that the stannylenoid H_2SnLiF has three kinds of structures, namely, the p-complex structure, the three-membered ring structure, and the "classical" tetrahedral structure that are shown in Fig. 1. We noted that Qi et al. [49] optimize the structure of H_2SnLiF at the HF/3-21G level and their calculated results indicated that H_2SnLiF has four stable structures, namely, p-complex, three-membered ring configuration, σ-complex configuration, and "classical" tetrahedral configuration. However, the σ-complex configuration is not found at the M062X/def2-TZVP level in this work. The M062X/def2-TZVP calculated structural parameters such as bond length and bond angel are different from HF/3-21G calculated. Considering the level of the method and basis set, we believe the calculation results of M062X/def2-TZVP are more reliable. The relative energies are listed in Table 1. In the p-complex structure, the bond length of Sn–F and Sn–Li is 2.131 (2.149) and 2.573 (2.702) Å, respectively. Li is bonded to F, and the bond length is 1.720 (1.754) Å. The angle of ∠FSnLi is 41.6 (40.4)°. In the three-membered ring structure, the bond length of Sn–F and Sn–Li is 2.171 (2.144) and 2.663 (3.694) Å, respectively, which are longer than those in p-complex structure. Li is also bonded to F, and the bond length is 1.671 (1.716) Å, which is slightly shorter than that in the p-complex structure. The angle of ∠FSnLi

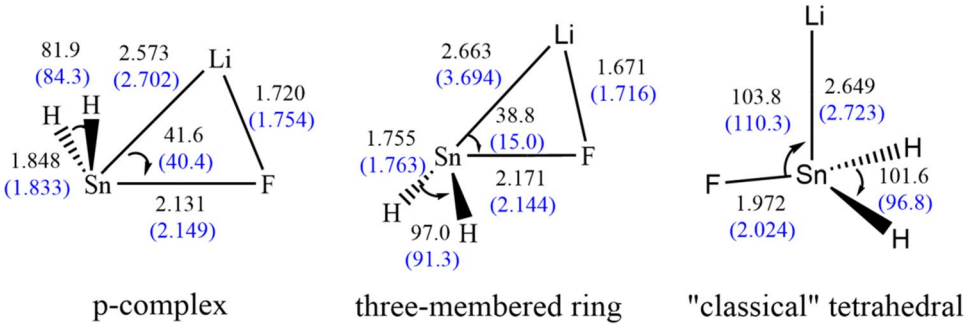

Fig. 1 The stable configuration of H_2SnLiF calculated at the level of M062X/def2-TZVP (bond length in Å, bond angle in degrees, and values in brackets are calculated in THF)

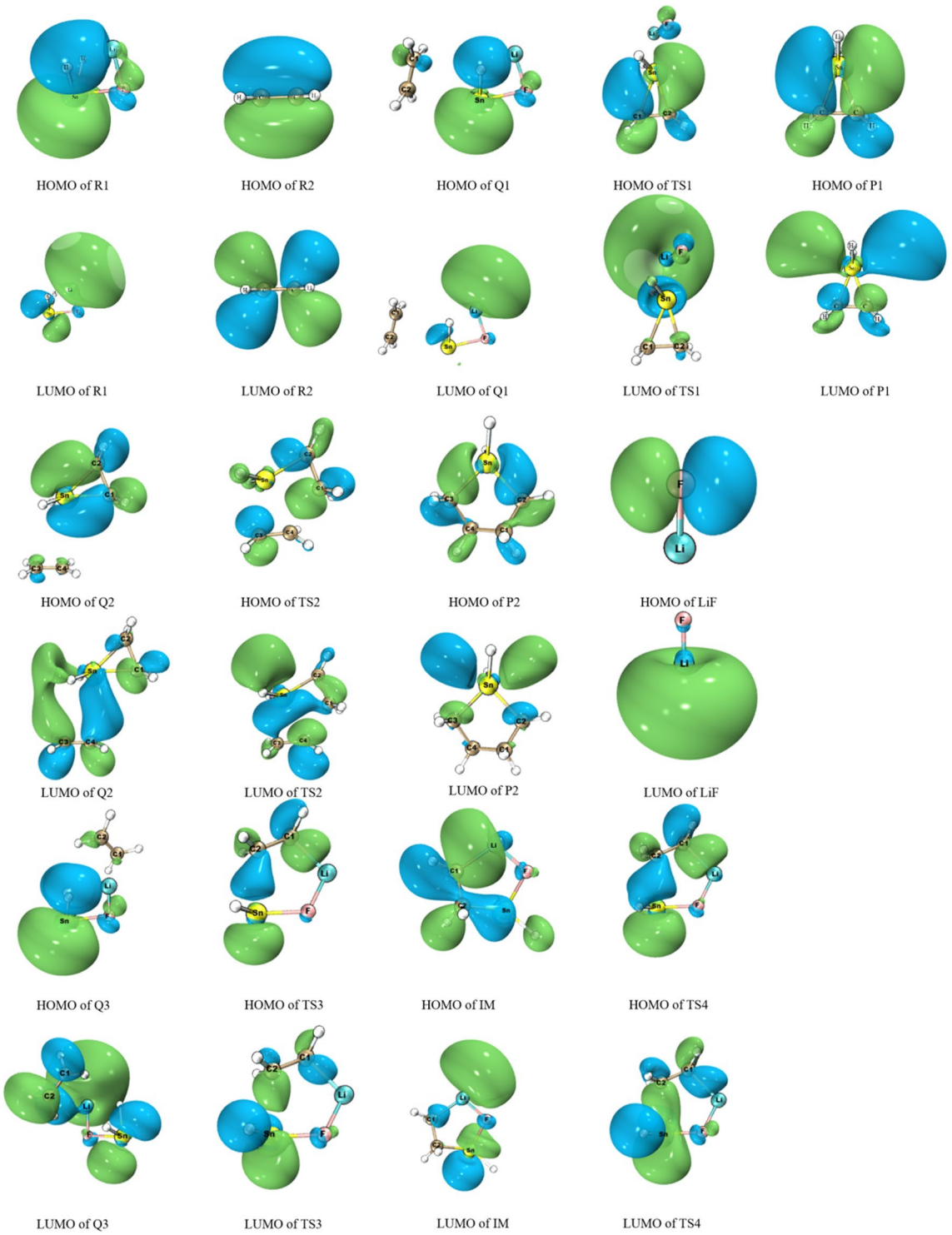

Fig. 2 Frontier molecular orbitals of stationary points on the potential energy surface calculated at M062X/def2-TZVP level

is 38.8 (15.0)°. The relative energy of the three-membered ring structure is 36.34 (4.19) kJ/mol. However, in the "classical" tetrahedral structure, Li and F are not bonded. The length of Sn–F is the shortest and that of Sn–Li is the longest. The relative energy of the "classical" tetrahedral one is 112.28 (54.64) kJ/mol. The data in brackets are the calculation results under THF solvent conditions, and the results are consistent with those under gas phase conditions. In the following discussions, only the reaction of the p-complex structure with ethylene is concerned.

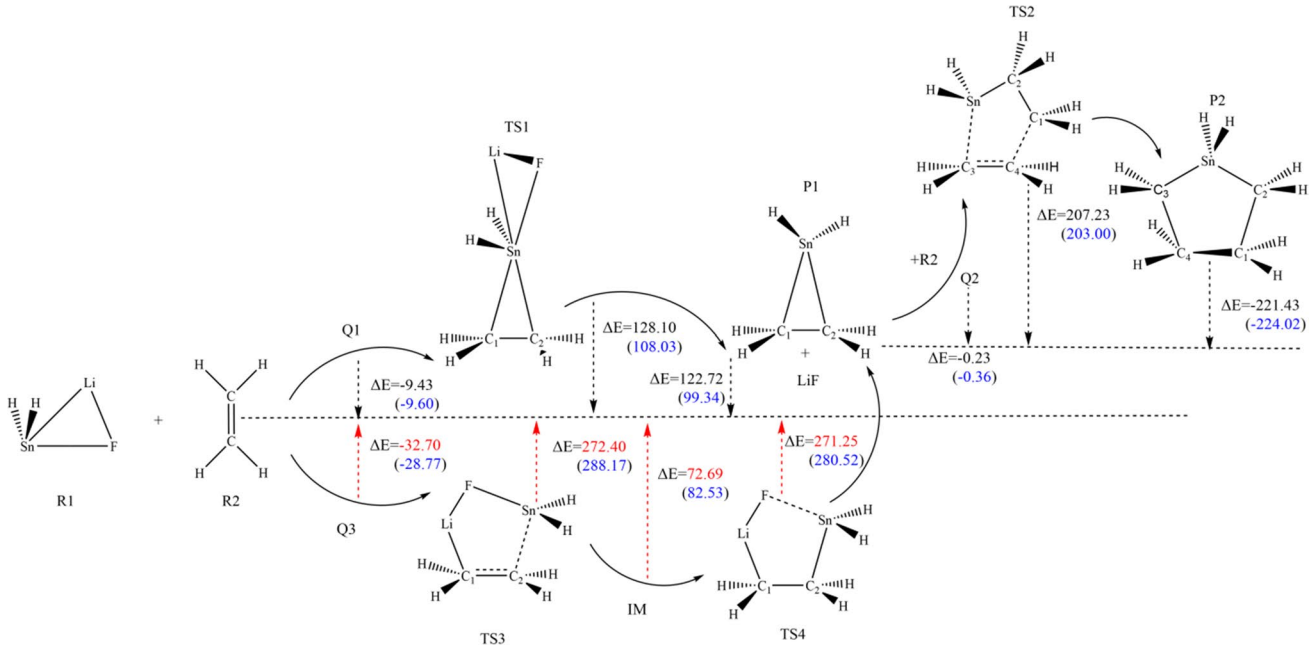

Fig. 3 Schematic diagram of two paths of addition reaction of H_2SnLiF with ethylene and relative energy of each stationary point on the potential energy surface (values in brackets are calculated in THF)

Reactions of H_2SnLiF and C_2H_4

The frontier molecular orbitals analysis of H_2SnLiF and C_2H_4 at the M062X/def2-TZVP level are shown in Fig. 2. The highest occupied molecular orbital of H_2SnLiF (R1) is concentrated in the Sn atom, while the lowest unoccupied molecular orbital is concentrated in the Li atom. The calculated results indicated that the addition reaction of H_2SnLiF with ethylene has two possible reaction paths along the potential energy surface: paths 1 and 2. As can be seen in Fig. 3, path 1 has a ternary ring transition state. After generating the initial product P1, it reacts with C_2H_4 (R2) for the second time, which has a five-membered ring transition state, and finally generates the five-membered ring product P2. There are two five-member ring transition states (TS3, TS4) and an intermediate state (IM) in path 2, which eventually produces P1, the same product as the first reaction in path 1. The potential energy surfaces of the addition reaction are shown in Fig. 3; the relative energies are on the basis of the sum of the energies of $H_2SnLiF + C_2H_4$ and $P1+C_2H_4$. The optimized geometries of each structure on the potential energy surface of the addition reaction including reactant (R), precursor complex (Q), transition state (TS), intermediate (IM), and product (P) are shown in Fig. 4.

Path 1

In path 1, when the stannylenoid H_2SnLiF and ethylene are near, the π* orbital (LUMO) of R2 attacks the σ orbital (HOMO) on the Sn atom, promoting the formation of the precursor complex (Q1). As can be seen in Fig. 4, the H_2SnLiF part of the complex did not change much from the structure of the leaving part, and the distances of Sn–C1 and Sn–C2 were 3.331 and 3.191 Å, respectively. The relative energy of Q1 is − 9.43 kJ/mol.

As R2 gets closer to the σ orbital on the Sn atom, the σ electron is partially donated into the antibonded π* orbital of R2 to reach the transition state (TS1). In Fig. 3, one can clearly see that path 1 involves a ternary ring, TS1. In TS1, the lengths of the Sn–C1 and Sn–C2 bonds are very short. The Sn–C1 bond length is 2.282 Å, which is 1.049 Å shorter than Q1, and the Sn–C2 bond length is 2.159 Å, which is 1.032 Å shorter than Q1. Meanwhile, the bond lengths of Sn–F and Sn–Li are further extended, being approximately 0.234 and 0.291 Å longer than the corresponding bond lengths in Q1, respectively. The above changes in bond length indicate that the Li–F part will leave the Sn atom of H_2SnLiF and subsequently form the products P1 and LiF.

As shown in Fig. 3, the relative energy of TS1 is 128.10 kJ/mol. Therefore, the first-step reaction potential barrier height for path 1 is approximately 137.53 kJ/mol. Frequency analysis calculations performed at the M062X/def2-TZVP level of theory show that TS1 has a unique imaginary frequency (266.4 i cm^{-1}). IRC analysis shows that TS1 is the true transition state for the first step of the reaction of path 1 in the addition reaction of H_2SnLiF with C_2H_4, correctly connecting Q1,P1 and LiF. The relative

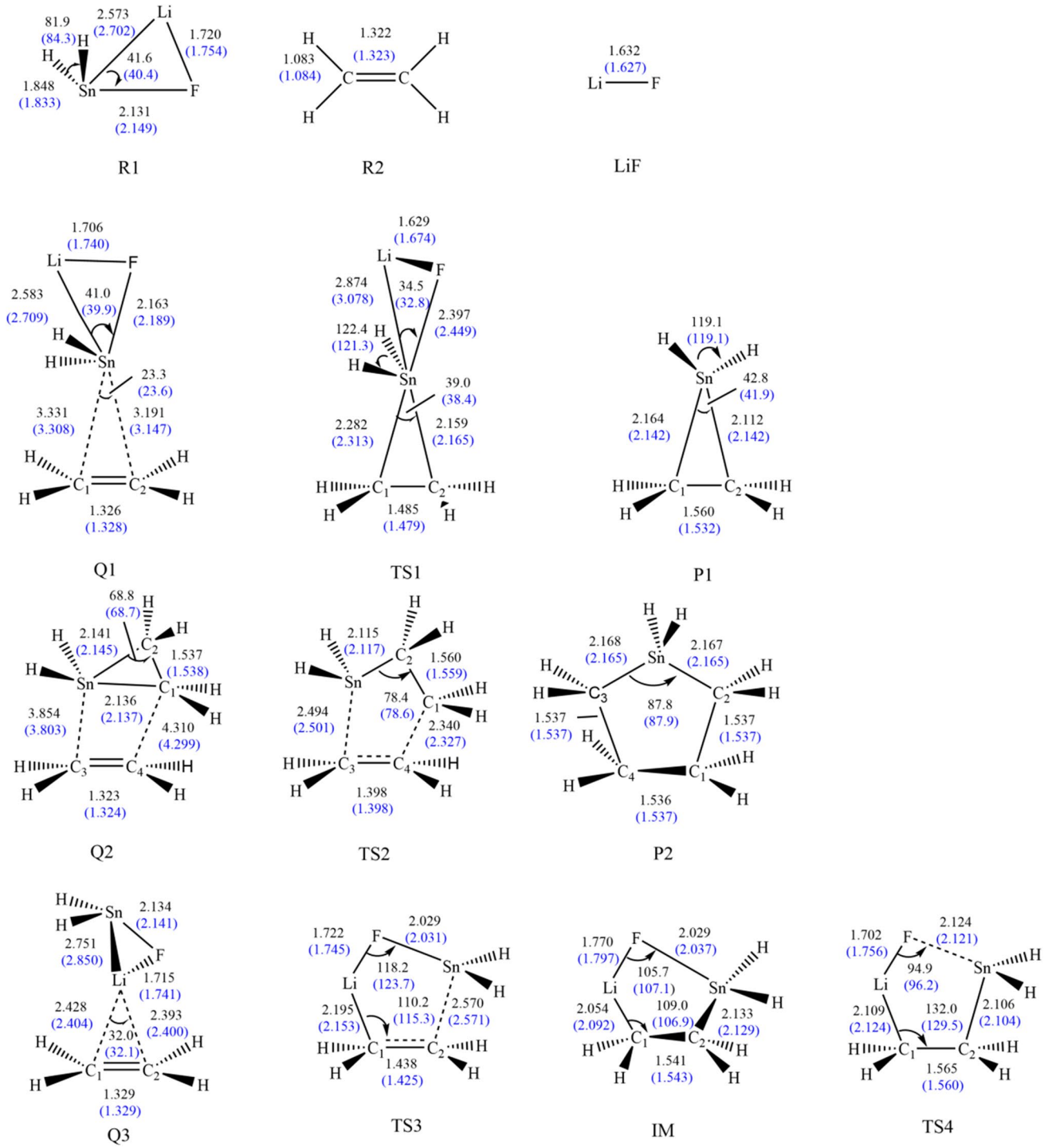

Fig. 4 Geometric configurations of the stationary points on the potential energy surface for the addition reaction of H_2SnLiF with ethylene were obtained at the M062X/def2-TZVP level (bond lengths in Å and values in brackets are calculated in THF)

energy of P1 and LiF is 122.72 kJ/mol, so the first step reaction is endothermic reaction.

In this case, the first step of the addition reaction in path 1 will occur, with the products being a tin-containing three-membered ring (P1) and LiF. After the formation of the product P1, P1 can continue to react with ethylene in a second step similar to the first step reaction. In the second step of the reaction in path 1, the antibonded π* orbital (LUMO) of R2 attacks the HOMO orbital (p orbital on the Sn atom and σ orbital on the C atom) in the product P1

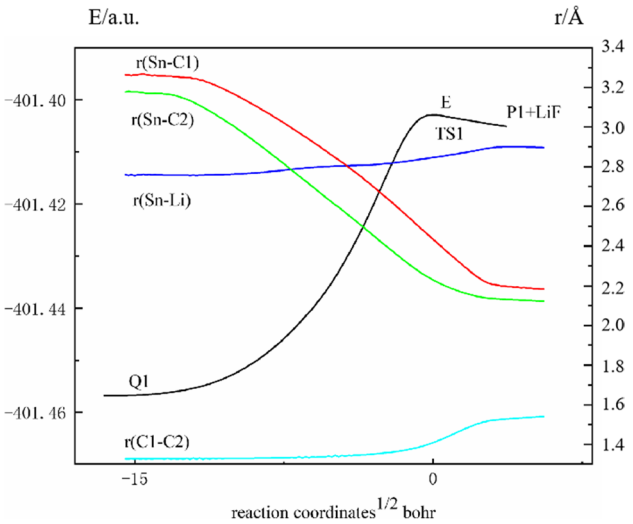

Fig. 5 The changes in energy and bond distances along the reaction coordinate of the first step of path 1

to form the precursor complex Q2. In Fig. 4, one can see that the distances of Sn–C1 and Sn–C2 in Q2 are not much different compared to P1, whose distances are 2.136 and 2.141 Å, respectively. The Sn–C3 and C1–C4 distances are 3.854 and 4.310 Å, respectively. The relative energy of Q2 is − 0.23 kJ/mol.

As R2 approaches further, the π electron on R2 is partially donated to the HOMO orbital of P1 to reach the transition state (TS2), and a transition state TS2 is formed at the potential energy surface of the addition reaction. In TS2, the distances of Sn–C3 and C1–C4 are 2.494 and 2.340 Å, respectively, compared to Q2, which are shortened by 1.360 and 1.970 Å, respectively, while the C1–C2

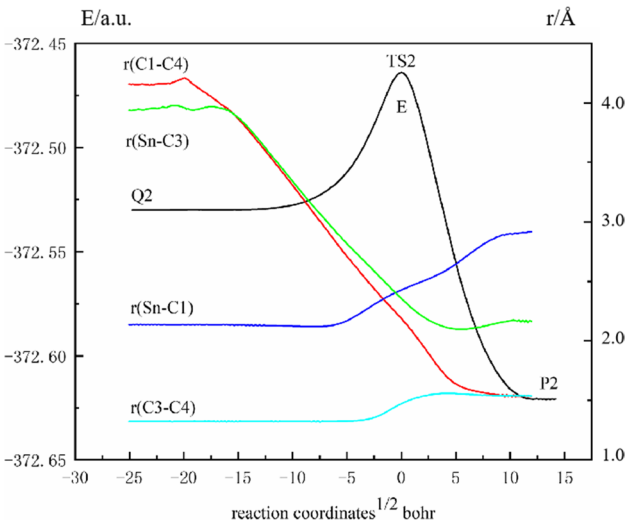

Fig. 6 The changes in energy and bond distances along the reaction coordinate of the second step of path 1

bond length is extended to 1.560 Å, and the Sn–C2–C1 bond angle is reduced by 9.6°. The change in bond length and bond angle indicates that P1 has partially combined with ethylene, and, as the reaction proceeds, the product P2 is produced.

The relative energy of TS2 is 207.23 kJ/mol; therefore, the barrier of the second step of path 1 is approximately 207.46 kJ/mol. The calculations show that TS2 has a unique imaginary frequency (655.6 i cm^{-1}), which is verified by IRC to be the correct and connects the precursor complex Q2 with the product P2 and is therefore the true transition state for the second step of the path 1. The relative energy of P2 is − 221.43 kJ/mol, indicating thermodynamically that the second step of the reaction is exothermic.

Path 2

In path 2, the precursor complex Q3 is formed when the π orbital (HOMO) of R2 attacks the σ orbital on the Li atom (LUMO). As can be seen in Fig. 4, in Q3, the Li atom is close to C1 and C2 atoms, and the distances of Li–C1 and Li–C2 are 2.428 and 2.393 Å, respectively. Compared with reactant, Sn–F bond and Sn–Li bond prolong by 0.1780 and 0.003 Å, respectively. As the reaction proceeds, R2 further approaches H_2SnLiF, and the π electron in R2 is partially donated to the LUMO of H_2SnLiF (σ orbital on the Li atom and p orbital of the Si atom) to reach the transition state (TS3). The distance of Sn–C2 is 2.570 Å, and the bond length of Li–C1 is shortened to 2.195 Å. This indicates that the intermediate (IM) is about to form a five-membered ring. After the intermediate IM is formed, the energy gradually increases, the distance of Sn–F and Li–C1 bond extends to 2.124 and 2.109 Å, respectively. Then, another transition state, TS4, would be formed. The extension of Sn–F bond and Li–C1 bond indicates that LiF is about to leave.

The relative energies of Q3, TS3, IM, and TS4 are − 32.70, 272.40, 72.69, and 271.25 kJ/mol, respectively. Therefore, the reaction barrier of the second pathway for the addition reaction of H_2SnLiF with C_2H_4 is 305.10 kJ/mol. The M062X/def2-TZVP calculated imaginary frequencies of TS3 and TS4 are 925.5i and 152.2i cm^{-1}, respectively. It is verified by IRC calculations that TS3 correctly connects the precursor Q3 to the intermediate IM, and TS4 correctly connects IM to the product P1. Path 2 has a higher barrier than path 1, which means it is harder to add through path 2 than it is through path 1.

Mechanisms of addition reactions

As the addition reaction goes through two different pathways, the mechanisms are different according to the calculations. Therefore, we explain the mechanisms in each of these two pathways. Based on the optimized structures of

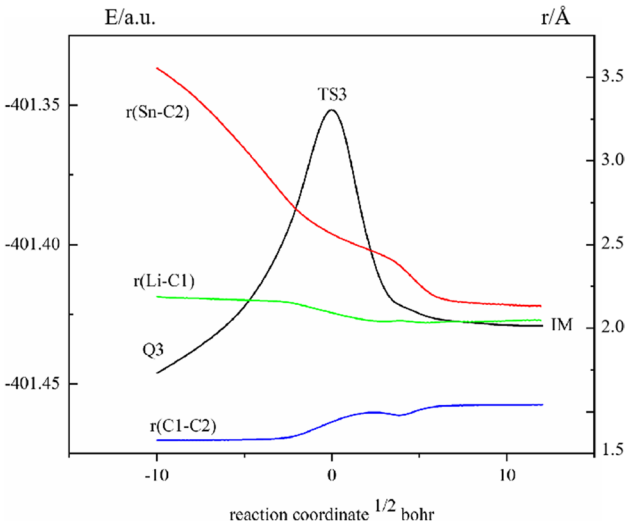

Fig. 7 The changes in energy and bond distances along the reaction coordinate of the first step (for TS3) of path 2

the transition states (TS1, TS2, TS3, and TS4), IRC analyses were calculated to investigate the interactions between the reactants H_2SnLiF and C_2H_4 during the addition reaction. The changes in energy and bond length along the IRC pathway are shown in Figs. 5, 6, 7, and 8.

In the first step of the reaction in path 1, as shown in Fig. 5, the energy increases sharply in this region of the reaction coordinates from – 15 to 0 and reaches a maximum at point 0. Within this region, the bond lengths of Sn–Li and C1–C2 increase slightly but do not change much overall, while the distance between Sn–C1 and Sn–C2 is gradually decreasing. The decrease in the distance between Sn–C1 and Sn–C2 means that Sn–C1 and Sn–C2 may form new bonds.

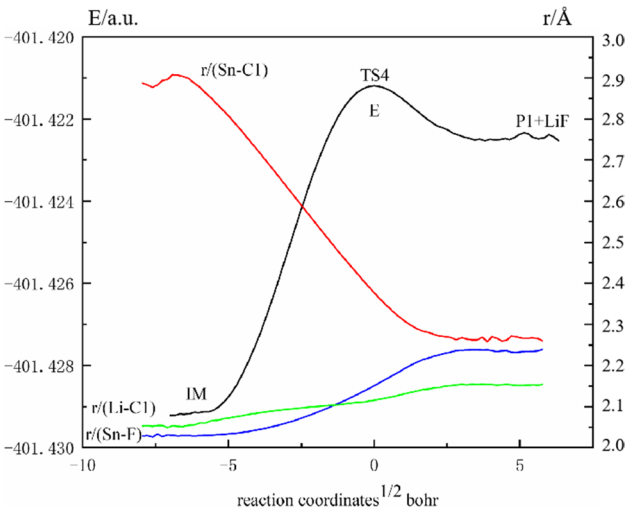

Fig. 8 The changes in energy and bond distances along the reaction coordinate of the second step (for TS4) of path 2

After the 0 point, the energy starts to decrease, and in this region the bond lengths of Sn–Li and C1–C2 continue to increase, while the distances between Sn–C1 and Sn–C2 continue to decrease, indicating the formation of a heterocyclic tin compound in the next process.

After the first step of the addition reaction, the reaction continues and the second step of the addition reaction occurs, as shown in Fig. 6. In this region of the reaction coordinate from – 25 to 0, the energy starts to increase and reaches a maximum at point 0. In this region, the distances of C1–C4 and Sn–C3 are continuously shortening, while the bond lengths of Sn–C1 and C3–C4 start to increase, which indicates that the C1–C4 and Sn–C3 bond energy will form a new bond and a possible break between the Sn–C1 and C3–C4 bonds. The reaction coordinates begin to drop sharply in energy after the 0 point, and the distances of C1–C4 and Sn–C3 continue to shorten, while similarly the Sn–C1 and C3–C4 bonds continue to elongate, indicating the imminent formation of a five-membered ring product.

Compared to path 1, the reaction mechanism of path 2 is different. It can be seen in Fig. 7 that the energy increases sharply in this region of the reaction coordinates from – 10 to point 0 and reaches a maximum at point 0. In this region, we can see that the distance of Sn–C2 is gradually shortened, the distance of Li–C1 is also shortened, and the bond length of C1–C2 is lengthened, which means that R1 and R2 are gradually close, and there is a tendency to form a five-membered ring. After 0 point, the energy of the system starts to decrease, the distance between Sn–C2 and Li–C1 is still shortening, and the bond length of C1–C2 is lengthening and finally tends to remain unchanged. At this time, the intermediate IM has been formed. After the intermediate is formed, it can be seen in Fig. 8 that the system energy is increasing in the range of – 10 to 0, and with the shortening of the distance between Sn atoms and C1 atoms and the extension of Li–C1 and Sn–F bonds, it proves that Li–C1 and Sn–F bonds are about to break, and a new bond is about to form between Sn and C1 atoms. After the point 0, the system energy decreases, the Li–C1 and Sn–F bonds are broken, the LiF leaves, and Sn–C1 bond is formed, forming a three-member ring product.

Solventing effect

In order to study the effect of solvent on the addition reaction of H_2SnLiF and ethylene, SMD model was used to set the addition reaction in THF solvent. All optimizations were performed at the M062X/def2-TZVP level, and single-point energy calculations were performed at the QCISD/def2-TZVP level. The relative energies and optimized geometries are also shown in Figs. 3 and 4. The calculated results indicated that the addition reaction in THF also passes through two paths: paths 1 and 2. The optimized geometries of all

the stationary points in THF are different from those in vacuum. The biggest difference in bond length value and bond angle value is 0.099 Å and 5.5°, respectively. As can be seen in Fig. 3, the first step reaction barrier height in THF is 117.63 kJ/mol for path 1 and 203.36 kJ/mol for the second step reaction, while in path 2 the addition reaction barrier is 316.94 kJ/mol, which means that path 1 is more likely to occur. Compared in vacuum, the potential barrier of path 1 in THF solvent is lowered, which means that the addition reaction of H_2SnLiF with ethylene is easier in THF solvent.

Conclusions

Addition reaction of H_2SnLiF with ethylene was investigated using the M062X and QCISD methods on density functional theory. The results show that the addition reaction goes through two different pathways, both in vacuum and in tetrahydrofuran solvent. Path 1 is a two-step reaction, with the first step producing the three-membered ring product, which is an exothermic reaction, followed by the three-membered ring product continuing the addition reaction with ethylene to produce the pentacyclic product, which is exothermic. Path 2 passes through two five-membered ring transition states along the potential energy surface to generate the same product as path 1. The calculated energy barriers for the two paths (the first step reaction of path 1 and the energy barrier of path 2) are 137.53 and 305.10 kJ/mol, respectively, and the second step reaction of path 1 has a potential barrier of 207.46 kJ/mol. Therefore, path 1 is more favorable than path 2. In THF solution, the addition reaction is more likely to occur. All calculations show that stannylenoid H_2SnLiF can promote similar cyclopropanoid reactions and can be further cyclized to produce five-membered cycloproducts. This work provides a new way for synthesis of tin heterocyclic compounds.

Author contribution All authors contributed to the study conception and design. Shuo Wu and Bingfei Yan wrote the main manuscript text. Shaoli Liu and Wenzuo Li edited and revised the manuscript of the article. All authors reviewed the manuscript.

Funding This research was supported by the National Natural Science Foundation Committee of China (No. 21103145), the Natural Science Foundation of Shandong Province (No. ZR2016BM23), and the Special Foundation of Youth Academic Backbone of Yantai University.

Data availability All data generated or analyzed during this study are included in this published article.

Declarations

Competing interests The authors declare no competing interests.

References

1. Boche G, Lohrenz JCW (2001) The electrophilic nature of carbenoids, nitrenoids, and oxenoids. J Chem Rev 101:697–756. https://doi.org/10.1021/cr940260x
2. Rappoport Z, Marek I eds (2004) The chemistry of organolithium compounds. John Wiley & Sons. https://doi.org/10.1002/047002111X
3. Nozakura S, Konotsune S (1956) Cyanoethylation of trichlorosilane. I. β-Addition. J J Bull Chem Soc Japan 29:322–326. https://doi.org/10.1246/bcsj.29.322
4. Zon G, DeBruin KE, Naumann K et al (1969) Stereospecific desulfurization of acyclic phosphine sulfides with hexachlorodisilane and the alkaline hydrolysis of monoalkoxy-and monoalkylthiophosphonium salts. J J Amer Chem Soc 91:7023–7027. https://doi.org/10.1021/ja01053a022
5. Oehme H, Weiss H (1987) Reaction of 2,4,6-tri-t-butylphenyllithium with bromotrichlorosilane. Generation of trichlorosilyllithium, LiSiCl3. J Organomet Chem 319:C16–C18. https://doi.org/10.1016/0022-328X(87)80359-5
6. Kawachi A, Tamao K (1997) Preparations and reactions of functionalized silyllithiums. J Bull Chem Soc Japan 70:945–955. https://doi.org/10.1246/bcsj.70.945
7. Tamao K, Kawachi A, Asahara M et al (1999) Recent developments in silicon interelement linkage: the case of functionalized silyllithium, silylenoid and sila-ylide. J Pur App Chem 71:393–400. https://doi.org/10.1351/pac199971030393
8. Tokitoh N, Hatano K, Sadahiro T et al (1999) Generation and reactions of an overcrowded diaryldilithiosilane. J Chem Lett 28:931–932. https://doi.org/10.1246/cl.1999.931
9. Kawachi A, Tamao K (2000) Structures of [(amino) phenylsilyl] lithiums and related compounds in solution and in the solid state. J J Amer Chem Soc 122:1919–1926. https://doi.org/10.1021/ja993101+
10. Fischer R, Baumgartner J, Kickelbick G et al (2003) The first stable β-fluorosilylanion. J J Amer Chem Soc 125:3414–3415. https://doi.org/10.1021/ja0291639
11. Lee ME, Cho HM, Lim YM et al (2004) Syntheses and reactivities of stable halosilylenoids,(Tsi)X2SiLi(Tsi=C(SiMe3)3, X= Br,Cl). J Chem–A Europ J 10:377–381. https://doi.org/10.1002/chem.200305151
12. Molev G, Bravo-Zhivotovskii D, Karni M et al (2006) Synthesis, molecular structure, and reactivity of the isolable silylenoid with a tricoordinate silicon. J J Amer Chem Soc 128:2784–2785. https://doi.org/10.1021/ja0575880
13. Cho HM, Lim YM, Lee ME (2010) Reactivities of chlorotrisylsilylenoid with ketones. J Dalton Trans 39:9232–9234. https://doi.org/10.1039/C0DT00147C
14. Lim YM, Park CH, Yoon SJ et al (2010) New synthetic routes for silaheterocycles: reactions of a chlorosilylenoid with aldehydes. J Organometallics 29:1355–1361. https://doi.org/10.1021/om9008789
15. Cho HM, Bok K, Park SH et al (2012) A new synthetic route for silacyclopropanes: reactions of a bromosilylenoid with olefins. J Organometallics 31:5227–5230. https://doi.org/10.1021/om3005349
16. Song JH, Park SH, Cho HM et al (2015) Reactivity of bromosilylenoid with heterocumulenes. J J Organometallic Chem 799:128–131. https://doi.org/10.1016/j.jorganchem.2015.09.016
17. Clark T, von Ragué SP (1980) The isomeric structures of SiH-2LiF. J J Organometallic Chem 191:347–353. https://doi.org/10.1016/S0022-328X(00)81063-3
18. Feng S, Feng D, Deng C (1993) Theoretical studies on the structures and reactivity of silylenoids. III. The structures and

isomerization of silylenoid H2SiNaF. J Chem Phys Lett 214:97–102. https://doi.org/10.1016/0009-2614(93)85461-V
19. Tanaka Y, Hada M, Kawachi A et al (1998) Self-condensation reaction of lithium (alkoxy) silylenoid: a model study by ab initio calculation. J Organometallics 17:4573–4577. https://doi.org/10.1021/om980567c
20. Feng S, Feng D, Li J (2000) An ab initio study on the insertion reaction of silylenoid H2SiLiF with H2. J Chem Phys Lett 316:146–150. https://doi.org/10.1016/S0009-2614(99)01269-5
21. Xie J, Feng D, Feng S (2007) Theoretical study on the substitution reactions of silylenoid H2SiLiF with CH4, NH3, H2O, HF, SiH4, PH3, H2S, and HCl. J J Phys Chem A 111:8475–8481. https://doi.org/10.1021/jp070773a
22. Zhang XL, Zhang MX, Yan BF et al (2020) A spiro-Ge-heterocyclic compound formation via germylenoid and formaldehyde: a theoretical study. J Russ J Phys Chem A 94:2084–2090. https://doi.org/10.1134/S0036024420100349
23. Li WZ, Cheng JB, Gong BA et al (2006) DFT study on the unsaturated germylenoid H2CGeNaF. J J Organometallic Chem 691:5984–5987. https://doi.org/10.1016/j.jorganchem.2006.09.028
24. Ohtaki T, Ando W (1996) Dichlorodigermacyclobutanes and digermabicyclo [2.2. 0] hexanes from the reactions of [tris (trimethylsilyl) methyl] chlorogermylene with olefins. J Organometallics 15:3103–3105. https://doi.org/10.1021/om9600147
25. Filippou AC, Stumpf KW, Chernov O et al (2012) Metal activation of a germylenoid, a new approach to metal–germanium triple bonds: synthesis and reactions of the germylidyne complexes [Cp(CO)2MGe–C(SiMe3)3](M= Mo, W). J Organometallics 31:748–755. https://doi.org/10.1021/om201176n
26. Suzuki Y, Sasamori T, Guo JD et al (2016) Frontispiece: isolation and ambident reactivity of a chlorogermylenoid. J Chem–A Europ J 22. https://doi.org/10.1002/chem.201683961
27. Grugel C, Neumann WP, Sauer J et al (1978) A highly stereoselective C-C coupling of aldehydes forming glycols via a stannylenoid reaction. J Tetrahedron Lett 19:2847–2850. https://doi.org/10.1016/S0040-4039(01)94880-4
28. Arif AM, Cowley AH, Elkins TM (1987) A bulky silyl derivative of tin (II). J J Organometallic Chem 325:C11–C13. https://doi.org/10.1016/0022-328X(87)80413-8
29. Ochiai T, Franz D, Wu XN et al (2016) A tin analogue of carbenoid: isolation and reactivity of a lithium bis (imidazolin-2-imino) stannylenoid. J Angew Chem Int Ed 55:6983–6987. https://doi.org/10.1002/anie.201602178
30. Yan C, Li Z, Xiao XQ et al (2016) Reversible stannylenoid formation from the corresponding stannylene and cesium fluoride. J Angew Chem Int Ed 55:14784–14787. https://doi.org/10.1002/anie.201608162
31. Gross LW, Moser R, Neumann WP et al (1982) Insertion reactions of thermally generated stannylenes R2Sn into Sn-X (X= Cl, Br, SPh) and Sn-Sn bonds. J Tetrahedron Lett 23:635–638. https://doi.org/10.1016/S0040-4039(00)86909-9
32. Fu J, Neumann WP (1984) Organozinnverbindungen: XXX. Über das hexa-9-phenantryl-cyclotristannan. J J Organometallic Chemistry 272:C5–C9. https://doi.org/10.1016/0022-328X(84)80448-9
33. Klinkhammer K (2002) Dihypersilylstannylene and dihypersilylplumbylene—two Lewis-amphoteric carbene homologues. J Polyhedron 21:587–598. https://doi.org/10.1016/S0277-5387(01)01029-4
34. Zhao H, Li J, Xiao XQ et al (2018) Cation-triggered stannate (ii)/stannylenoid/stannylene conversion. J Chem–A Europ J 24:5967–5973. https://doi.org/10.1002/chem.201800602
35. Yan L, Yan C, Xu J et al (2021) Diverse reactions of a fluorostannylenoid towards ethynes. J Dalton Trans 50(31):10806–10810. https://doi.org/10.1039/D1DT01914G
36. Zhao XX, Fujimori S, Kelly JA et al (2022) Isolation and reactivity of stannylenoids stabilized by amido/imino ligands. J Chem–A Europ J 2023: e202202712. https://doi.org/10.1002/chem.202202712
37. Molander GA, Harring LS (1989) Samarium-promoted cyclopropanation of allylic alcohols. J J Org Chem 54:3525–3532. https://doi.org/10.1021/jo00276a008
38. Hermann H, Lohrenz JCW, Kühn A et al (2000) The influence of the leaving group X (X= F, Cl, Br, I, OH) on the carbenoid nature of the carbenoids LiCH2X and XZnCH2X—A theoretical study. J Tetrahedron 56:4109–4115. https://doi.org/10.1016/S0040-4020(00)00334-3
39. Nakamura M, Hirai A, Nakamura E (2003) Reaction pathways of the Simmons− Smith reaction. J J Amer Chem Soc 125:2341–2350. https://doi.org/10.1021/ja026709i
40. Li ZH, Ke Z, Zhao C et al (2006) A density functional theory study of aluminum carbenoid (CH3)2AlCH2X (X= Cl, Br, I) promoted cyclopropanation reactions compared to IMCH2I (M= Li, Sm, Zn) carbenoids. J Organometallics 25:3735–3742. https://doi.org/10.1021/om060333q
41. Li ZH, Geng ZY, Zhao C et al (2007) The influence of the leaving group X (X= F, Cl, Br, I) on the carbenoid nature of the carbenoids X2AlCH2X–A theoretical study. J J Molec Struct: Theochem 807:173–178. https://doi.org/10.1016/j.theochem.2006.12.034
42. Parr RG, Yang W (1989) International series of monographs on chemistry 16: density-functional theory of atoms and molecules. New York Oxford University Press
43. Seminario JM (Ed.) (1996) Recent developments and applications of modern density functional theory. https://doi.org/10.1016/s1380-7323(96)x8058-0
44. Gauss J, Cremer D (1988) Analytical evaluation of energy gradients in quadratic configuration interaction theory. J Che Phys Lett 150:280–286. https://doi.org/10.1016/0009-2614(88)80042-3
45. Marenich AV, Cramer CJ, Truhlar DG (2009) Performance of SM6, SM8, and SMD on the SAMPL1 test set for the prediction of small-molecule solvation free energies. J J Phys Chem B 113:4538–4543. https://doi.org/10.1021/jp809094y
46. Humphrey W, Dalke A, Schulten K (1996) VMD: visual molecular dynamics. J J Mol Graph 14:33–38. https://doi.org/10.1016/0263-7855(96)00018-5
47. Lu T, Chen F (2012) Multiwfn: A multifunctional wavefunction analyzer. J J Comput Chem 33:580–592. https://doi.org/10.1002/jcc.22885
48. Frisch MJ, Trucks GW, Schlegel HB et al (2003) Revision B. Gaussian. J Inc., Pittsburgh PA
49. Hua-Yu Q, Cong-Hao D (1996) Theoretical studies on the structures and reactivity of stannylenoids I. The structures and isomerization of stannylenoid H2SnLiF. J Chin J Chem 14:310–314. https://doi.org/10.1002/cjoc.19960140405